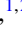





# Heat capacity of nonequilibrium electron-hole plasma in graphene layers and graphene bilayers

V. Ryzhii <sup>1,2,3</sup>, M. Ryzhii,<sup>4</sup> T. Otsuji <sup>1</sup>, V. Mitin <sup>5</sup>, and M. S. Shur <sup>6</sup>

<sup>1</sup>Research Institute of Electrical Communication, Tohoku University, Sendai 980-8577, Japan

<sup>2</sup>Institute of Ultra High Frequency Semiconductor Electronics of RAS, Moscow 117105, Russia

<sup>3</sup>Center for Photonics and Two-Dimensional Materials, Moscow Institute of Physics and Technology, Dolgoprudny 141700, Russia

<sup>4</sup>Department of Computer Science and Engineering, University of Aizu, Aizu-Wakamatsu 965-8580, Japan

<sup>5</sup>Department of Electrical Engineering, University at Buffalo, SUNY, Buffalo, New York 1460-1920, USA

<sup>6</sup>Department of Electrical, Computer, and Systems Engineering, Rensselaer Polytechnic Institute, Troy, New York 12180, USA



(Received 6 November 2020; revised 29 May 2021; accepted 4 June 2021; published 11 June 2021)

We analyze the statistical characteristics of quasinequilibrium two-dimensional electron-hole plasmas in graphene layers (GLs) and graphene bilayers (GBLs) and evaluate their heat capacity. The GL heat capacity of the weakly pumped intrinsic or weakly doped GLs normalized by the Boltzmann constant is equal to  $c_{\text{GL}} \simeq 6.58$ . With varying carrier temperature the intrinsic GBL carrier heat capacity  $c_{\text{GBL}}$  changes from  $c_{\text{GBL}} \simeq 2.37$  at  $T \lesssim 300$  K to  $c_{\text{GBL}} \simeq 6.58$  at elevated temperatures. These values are markedly different from the heat capacity of classical two-dimensional carriers with  $c = 1$ . The obtained results can be useful for the optimization of different GL- and GBL-based high-speed devices.

DOI: [10.1103/PhysRevB.103.245414](https://doi.org/10.1103/PhysRevB.103.245414)

## I. INTRODUCTION

The properties of the graphene layers (GLs) and graphene bilayers (GBLs), in particular, their optical characteristics, conductivity, plasmonic properties, thermal conductivity (both associated with the lattice and the carriers), heat capacity, and others, have been extensively studied theoretically and experimentally [1–19] (see the references therein). The contributions of the carriers in GLs and GBLs to the overall heat capacity are small in comparison with the contributions of the lattice vibrations [20]. However, the electron and hole heat capacity determines the rate of carrier heating and cooling. This heating/cooling rate affects the ultimate high-speed performance, including the dynamic response and the modulation characteristics of the GL- and GBL-based devices using a variation of the two-dimensional electron-hole plasma (2DEHP) parameters (such as the effective carrier temperature, conductivity, and transparency of the incident radiation). Such GL and GBL devices include the carrier bolometric detectors [21,22], electro-optical modulators [23], fast thermal radiation emitters [24–31], and superluminescent and lasing diodes [32]. Many papers deal with the theoretical evaluation of the GL- and GBL-lattice heat capacity (see, for example, a recent review [19]). However, the carrier capacity of the intrinsic quasinequilibrium 2DEHP in GLs and GBLs was not addressed. The case of highly doped GLs was briefly discussed in Refs. [33,34]. In this paper, we calculate the heat capacity of the 2DEHP in the equilibrium and of the 2DEHP somewhat deviating from the equilibrium due to the radiation absorption and/or the carrier injection.

## II. GENERAL RELATIONS

The dispersion relations for electrons (upper sign) and holes (lower sign) in the GLs and GBLs are presented as

$$\varepsilon_{\text{GL}}^{\pm} = \pm v_W p, \quad \varepsilon_{\text{GBL}}^{\pm} \simeq \pm \frac{\gamma_1}{2} \left[ \sqrt{1 + 4v_W^2 p^2 / \gamma_1^2} - 1 \right]. \quad (1)$$

Here,  $\hbar$  is the Planck constant,  $v_W \simeq 10^8$  cm/s is the characteristic carrier velocity in GL and GBLs,  $p = |p|$  is the carrier momentum, and  $\gamma_1 \simeq 0.4$  eV is the band parameter (the GBL hopping parameter) [35,36]. Since the main contributions to the 2DEHP energy are given by the electrons and holes located not too far from the Dirac point, Eqs. (1) adequately describe their dynamics (see, however, Sec. IV, where the carrier dispersion law renormalization associated with the intercarrier interactions is discussed).

The electron-electron, electron-hole, and hole-hole interactions in GLs and GBLs are sufficiently strong in a wide range of 2DEHP densities (see, for example, Refs. [37–41]), so that the pertinent characteristic times  $\tau_{ee}$ ,  $\tau_{eh}$ , and  $\tau_{hh}$  are shorter or much shorter than the relaxation times related to scattering on impurities, optical phonons, and recombination. This enables effective carrier Maxwellization (Fermization) and, therefore, the formation in the 2DEHP of the electron and hole systems described by quasi-Fermi energy distribution functions  $f_e(\varepsilon)$  and  $f_h(\varepsilon)$  with a common effective temperature  $T$ ,  $f_e(\varepsilon) = [1 + \exp(\frac{\varepsilon - \mu_e}{k_B T})]^{-1}$  and  $f_h(\varepsilon) = [1 + \exp(\frac{\varepsilon - \mu_h}{k_B T})]^{-1}$ , where  $k_B$  is the Boltzmann constant,  $\varepsilon \geq 0$  is the carrier kinetic energy, and  $\mu_e$  and  $\mu_h$  are the electron and hole quasi-Fermi energies, respectively. The quasi-Fermi energies are counted from the Dirac point. In the undoped GLs and GBLs,  $\mu_e = \mu_h = 0$ , and the 2DEHP Fermi level coincides with the Dirac point. If the GL (or the GBL) is doped by donors,  $\mu_e > 0$ , while  $\mu_h < 0$ . In the equilibrium, i.e., without optical or injection pumping and with no heating of the 2DEHP by the electric field,  $\mu_e + \mu_h = 0$ , with the common Fermi level  $\zeta_F > 0$  in the conduction band. In this case,  $\mu_e$  and consequently  $\mu_h$  are determined by the donor sheet density  $\Sigma_d$ . In the acceptor doped GLs (GBLs),  $\mu_h > 0$  and  $\mu_e < 0$  with the Fermi level  $\zeta_F < 0$  in the valence band and  $\mu_h$  and  $\mu_e$  determined by the acceptor density  $\Sigma_a$ .

Due to the symmetry of the electron and hole dispersion relations given by Eq. (1), the 2DEHP in the undoped GLs and GBLs in equilibrium is symmetrical. In the case of interband pumping or heating by the electric field, the 2DEHP remains symmetrical even though it can be even far from equilibrium. Although the frequent electron-electron, electron-hole, and hole-hole collisions establish the common effective temperature for both the electron and hole components of the 2DEHP driven from equilibrium, the values of their quasi-Fermi energies  $\mu_e$  and  $\mu_h$  being equal to each other but *generally* not equal to zero ( $\mu_e = \mu_h = \mu \neq 0$ ), the electron and hole quasi-Fermi levels generally do not coincide (split).

The value of the combined quasi-Fermi energy  $\mu$  depends on (1) the method of forcing the 2DEHP away from equilibrium (for example, the interband generation of the electron-hole pairs and heating by dc or ac electric fields) and (2) the efficiency of the interband electron-hole generation and recombination associated with the optical phonon emission and absorption and the Auger processes (including those with the participation of impurities, acoustic phonons, etc. [14,42]).

The case  $\mu_e + \mu_h = 2\mu > k_B T$  is related to the pronounced interband population inversion in GLs and GBLs [14] (and the references therein). In such a situation, the quasi-Fermi levels of the electrons and holes split. The electron quasi-Fermi level might be in the conduction band, while the hole level is in the valence band. The latter can be achieved at a strong optical pumping or double injection leading to the generation of *low-energy* electron-hole pairs. In this case, an increase in the effective temperature due to the absorption of the incident photons or due to the injected electron-hole pairs is *slower* than an increase in the 2DEHP density. Even the 2DEHP cooling down is possible if the energy of the generated electron-hole pairs is smaller than the optical phonon energy. This reinforces the degeneration of the both electron and hole components. Such situations correspond to the formation of the interband population inversion and can be used for the realization of graphene-based interband terahertz and far infrared lasers (see, for example, Refs. [7,14] and references therein).

The Auger processes try to prevent the quasi-Fermi levels from splitting and the population inversion reducing of quasi-Fermi levels split, i.e., establishing the tendency of  $\mu_e + \mu_h = 2\mu \rightarrow 0$ . The realization or suppression of the population inversion or the suppression of the latter depends on the relative efficiency of the Auger generation-recombination processes and similar processes associated with the optical phonons.

The situation differs in GLs and GBLs. The standard lowest-order Auger processes in GLs are formally suppressed due to the one-dimensional character of the intercarrier collisions [43]. A detailed study of the Auger processes in graphene demonstrated [42] that the Auger processes associated with the lifting of the one-dimensional scattering limitations imposed by the energy and momentum conservation laws [14,42,43] can contribute to the general pattern of the generation-recombination processes. Moreover, the role of the Auger processes can be both moderate or sufficiently strong depending on the temperature, dielectric constant of the surrounded layers, and the presence or absence of highly conducting gates. In particular, the characteristic time  $\tau_A$  of the Auger recombination in GLs being about  $\tau_A \sim (1-10)$  ps

at the 2DEHP effective temperature  $\lesssim 300$  K can be about  $\tau_A \sim (50-100)$  fs at  $T = 1000-3000$  K [42].

In contrast, the 2DEHP degeneracy can be effectively lifted at the optical pumping or injection of high-energy carriers leading to high effective temperatures  $T$ , resulting in relatively small values of  $\mu$ . Such situations take place, for example, in both the electric-field [24-30] and vertical injection [31] driven GL-based thermal radiation sources.

The net carrier (electrons and holes) densities,  $\Sigma_{GL}$  and  $\Sigma_{GBL}$ , in the GL and GBL, respectively, in line with Eq. (1) are given by

$$\begin{aligned} \Sigma_{GL} &= \frac{2}{\pi \hbar^2 v_W^2} \int_0^\infty d\varepsilon \varepsilon \\ &\times \left[ \frac{1}{1 + \exp\left(\frac{\varepsilon - \mu_e}{k_B T}\right)} + \frac{1}{1 + \exp\left(\frac{\varepsilon - \mu_h}{k_B T}\right)} \right] \\ &= \frac{2(k_B T)^2}{\pi \hbar^2 v_W^2} \left[ \mathcal{F}_1\left(\frac{\mu_e}{k_B T}\right) + \mathcal{F}_1\left(\frac{\mu_h}{k_B T}\right) \right] \end{aligned} \quad (2)$$

and

$$\begin{aligned} \Sigma_{GBL} &= \frac{2}{\pi \hbar^2 v_W^2} \int_0^\infty d\varepsilon (\varepsilon + \gamma_1/2) \\ &\times \left[ \frac{1}{1 + \exp\left(\frac{\varepsilon - \mu_e}{k_B T}\right)} + \frac{1}{1 + \exp\left(\frac{\varepsilon - \mu_h}{k_B T}\right)} \right] \\ &= \frac{2}{\pi \hbar^2 v_W^2} \left[ \mathcal{F}_1\left(\frac{\mu_e}{k_B T}\right) + \mathcal{F}_1\left(\frac{\mu_h}{k_B T}\right) \right. \\ &\quad \left. + \frac{\gamma_1}{k_B T} \mathcal{F}_0\left(\frac{\mu_e}{k_B T}\right) + \frac{\gamma_1}{k_B T} \mathcal{F}_0\left(\frac{\mu_h}{k_B T}\right) \right]. \end{aligned} \quad (3)$$

Here,  $\mathcal{F}_\xi(y)$  is the Fermi-Dirac integral.

The carrier energy in the 2DEHP can be calculated as

$$\begin{aligned} \mathcal{E}_{GL} &= \frac{2}{\pi \hbar^2 v_W^2} \int_0^\infty d\varepsilon \varepsilon^2 \\ &\times \left[ \frac{1}{1 + \exp\left(\frac{\varepsilon - \mu_e}{k_B T}\right)} + \frac{1}{1 + \exp\left(\frac{\varepsilon - \mu_h}{k_B T}\right)} \right] \\ &= \frac{2(k_B T)^2}{\pi \hbar^2 v_W^2} \left[ \mathcal{F}_2\left(\frac{\mu_e}{k_B T}\right) + \mathcal{F}_2\left(\frac{\mu_h}{k_B T}\right) \right] \end{aligned} \quad (4)$$

and

$$\begin{aligned} \mathcal{E}_{GBL} &= \frac{2}{\pi \hbar^2 v_W^2} \int_0^\infty d\varepsilon \varepsilon (\varepsilon + \gamma_1/2) \\ &\times \left[ \frac{1}{1 + \exp\left(\frac{\varepsilon - \mu_e}{k_B T}\right)} + \frac{1}{1 + \exp\left(\frac{\varepsilon - \mu_h}{k_B T}\right)} \right] \\ &= \frac{2}{\pi \hbar^2 v_W^2} \left[ \mathcal{F}_2\left(\frac{\mu_e}{k_B T}\right) + \mathcal{F}_2\left(\frac{\mu_h}{k_B T}\right) \right. \\ &\quad \left. + \frac{\gamma_1}{k_B T} \mathcal{F}_1\left(\frac{\mu_e}{k_B T}\right) + \frac{\gamma_1}{k_B T} \mathcal{F}_1\left(\frac{\mu_h}{k_B T}\right) \right]. \end{aligned} \quad (5)$$

### III. QUASINONEQUILIBRIUM 2DEHP IN UNDOPED GL AND GBL

We focus on the undoped symmetrically pumped 2DEHP ( $\mu_e = \mu_h$ ) for the following two situations:

(1) The 2DEHP, being close to equilibrium (at which  $\mu = \mu_e = \mu_h = 0$ ), is forced to slightly deviate from this state by a moderate illumination or double injection. In this situation, a possible variation of the quasi-Fermi energies can be both positive or negative (the electron Fermi level is in the valence band, while the hole Fermi level is in the conduction band, both not so far from the Dirac point), i.e.,  $\mu \ll k_B T$ .

(2) The 2DEHP is heated due to the optical or injection generation of the hot electron-hole pairs (with the energy exceeding the optical phonon energy  $\hbar\omega \simeq 0.2$  eV). In such a case, the interband generation-recombination processes and the electron and hole intraband energy relaxation associated with the optical phonon absorption and emission lead to the quasi-Fermi energy  $\mu < k_B T$  in a wide pumping range (as demonstrated by the calculations involving the equations governed the interband transitions and intraband transitions [14]). Other mechanisms, which could potentially affect the interband and intraband balances of the carrier density and effective temperature, such as interband radiative transitions, are weak in comparison with the optical phonon mediated transitions. The interband transitions involving acoustic phonons are kinematically forbidden [8,9] and the intraband energy relaxation on the acoustic phonons is also insignificant. Moreover, the Auger generation-recombination processes effectively providing in a hot 2DEHP small values of  $\mu/k_B T$ ,  $\mu/k_B T \propto \tau_A/\tau_0$ , suppress the degeneration of both 2DEHP components [14,31]. Here,  $\tau_0 \simeq 1$  ps is the characteristic time of the optical phonon spontaneous emission in GLs. Considering the data for  $\tau_A$  for a hot 2DEHP shown above (and in Ref. [42]), one can obtain  $\tau_A/\tau_0 \sim (5-10) \times 10^{-2}$ . Therefore, in the following we assume  $\mu < k_B T$ . One can expect that the latter inequality is also valid at a moderate pumping condition. Due to quasiparabolic electron and hole dispersion relations in GBLs and the absence of essential intercarrier limitations, the latter can be applicable to the symmetric GBLs for a number of situations. At  $\mu < k_B T$ , our results are also valid for weakly doped GLs and GBLs.

Considering this, Eqs. (2) and (3) yield well-known formulas for the carrier densities in GLs and GBLs:

$$\Sigma_{\text{GL}} = \left( \frac{k_B T}{\hbar v_W} \right)^2 \left( \frac{\pi}{3} + \frac{4 \ln 2}{\pi} \frac{\mu}{k_B T} \right), \quad (6)$$

$$\Sigma_{\text{GBL}} = \left( \frac{k_B T}{\hbar v_W} \right)^2 \times \left[ \frac{\pi}{3} + \frac{2 \ln 2}{\pi} \frac{\gamma_1}{k_B T} + \left( \frac{4 \ln 2}{\pi} + \frac{\gamma_1}{k_B T} \right) \frac{\mu}{k_B T} \right]. \quad (7)$$

Equations (4) and (5) result in the following expressions for the carrier thermal energy density (thermal energy per GL and GBL area) as a function of the carrier effective temperature  $T$

and the combined quasi-Fermi energy  $\mu$ ,

$$\mathcal{E}_{\text{GL}} \simeq \frac{2(k_B T)^3}{\pi \hbar^2 v_W^2} \left[ 3\zeta(3) + \frac{\pi^2}{3} \frac{\mu}{k_B T} \right], \quad (8)$$

$$\mathcal{E}_{\text{GBL}} \simeq \frac{2(k_B T)^3}{\pi \hbar^2 v_W^2} \left[ 3\zeta(3) + \frac{\pi^2}{12} \frac{\gamma_1}{k_B T} + \left( \frac{\pi^2}{3} + \ln 2 \frac{\gamma_1}{k_B T} \right) \frac{\mu}{k_B T} \right], \quad (9)$$

where  $\zeta(x)$  is the Riemann zeta function  $\zeta(3) \simeq 1.202$ .

Considering that the 2DEHP heat capacities in GLs and GBLs (per area) are defined as  $C_{\text{GL}} = d\mathcal{E}_{\text{GL}}/dT$  and  $C_{\text{GBL}} = d\mathcal{E}_{\text{GBL}}/dT$ , we obtain from Eqs. (8) and (9)

$$C_{\text{GL}} \simeq \frac{2(k_B T)^2}{\pi \hbar^2 v_W^2} \left[ 9\zeta(3) + \frac{2\pi^2}{3} \frac{\mu}{k_B T} \right] \simeq \frac{6.58\pi}{3} \left( \frac{k_B T}{\hbar v_W} \right)^2, \quad (10)$$

$$C_{\text{GBL}} \simeq \frac{2(k_B T)^2}{\pi \hbar^2 v_W^2} \left[ 9\zeta(3) + \frac{\pi^2}{6} \frac{\gamma_1}{k_B T} + \left( \frac{2\pi^2}{3} + \ln 2 \frac{\gamma_1}{T} \right) \frac{\mu}{k_B T} \right] \simeq \frac{\pi}{3} \left( \frac{k_B T}{\hbar v_W} \right)^2 \left( 6.57 + \frac{\gamma_1}{k_B T} \right). \quad (11)$$

Since in the 2DEHP under consideration  $\mu \ll k_B T$ , according to Eqs. (6) and (7),

$$\Sigma_{\text{GL}} \simeq \frac{\pi}{3} \left( \frac{k_B T}{\hbar v_W} \right)^2, \quad (12)$$

$$\Sigma_{\text{GBL}} \simeq \frac{\pi}{3} \left( \frac{k_B T}{\hbar v_W} \right)^2 \left( 1 + \frac{6 \ln 2}{\pi^2} \frac{\gamma_1}{k_B T} \right), \quad (13)$$

the pertinent heat capacitances,  $c_{\text{GL}} = C_{\text{GL}}/k_B \Sigma_{\text{GL}}$  and  $c_{\text{GBL}} = C_{\text{GBL}}/k_B \Sigma_{\text{GBL}}$  (normalized by  $k_B$ , i.e., in units of the Boltzmann constant), per one carrier are equal to

$$c_{\text{GL}} \simeq \frac{54\zeta(3)}{\pi^2} \simeq 6.58, \quad (14)$$

$$c_{\text{GBL}} \simeq \frac{\pi^2}{6 \ln 2} \left( \frac{1 + \frac{54\zeta(3)}{\pi^2} \frac{k_B T}{\gamma_1}}{1 + \frac{\pi^2}{6 \ln 2} \frac{k_T}{\gamma_1}} \right) \simeq 2.37 \left( \frac{1 + 6.58 \frac{k_B T}{\gamma_1}}{1 + 2.37 \frac{k_B T}{\gamma_1}} \right). \quad (15)$$

### IV. COMMENTS

At  $k_B T \ll \gamma_1$  ( $T \lesssim 300$  K), Eq. (13) yields  $c_{\text{GBL}} \simeq (\pi^2/6 \ln 2) \simeq 2.37$ . When  $T$  is rather high,  $c_{\text{GBL}}$  increases, tending to  $c_{\text{GBL}} \simeq 6.58$ . Figure 1 shows the temperature dependences of the energy densities  $\mathcal{E}_{\text{GL}}$  and  $\mathcal{E}_{\text{GBL}}$  and the heat capacities per one carrier  $c_{\text{GL}}$  and  $c_{\text{GBL}}$  calculated using Eqs. (10), (11), (14), and (15) for  $\mu = 0$  (equilibrium 2DEHP) assuming  $\gamma_1 = 0.4$  eV.

A noticeable deviation of the heat capacities  $c_{\text{GL}}$  and  $c_{\text{GBL}}$  from the classical value for nondegenerate 2D systems (i.e., from  $c = 1$ ) seen from Eqs. (14) and (15), is associated with the nonparabolicity of the carrier spectra in both GLs and GBLs. The nonparabolicity provides different densities of states (a linear in GLs and a linear rising from a constant

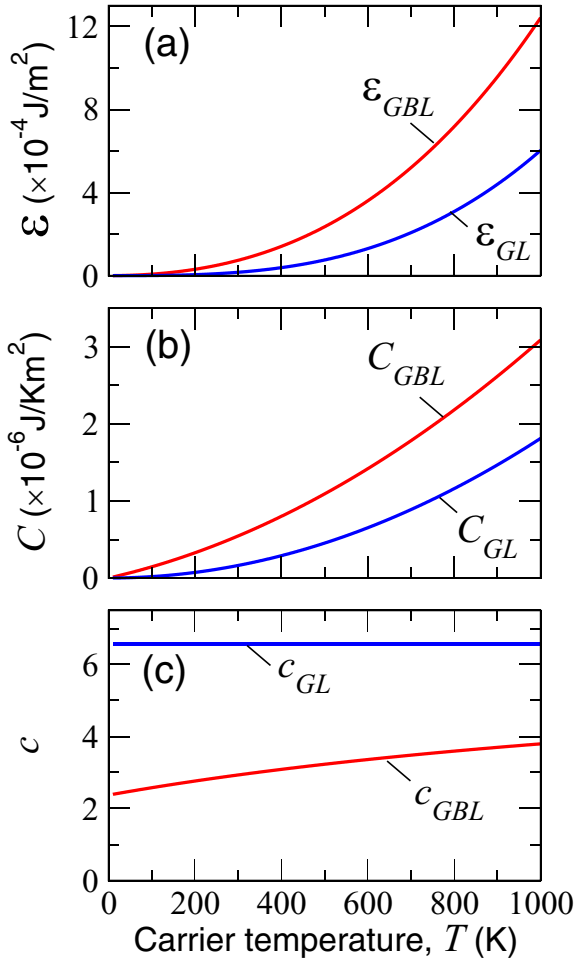


FIG. 1. The carrier (a) thermal energies  $\mathcal{E}_{GL}$  and  $\mathcal{E}_{GBL}$  per area, (b) heat capacities  $C_{GL}$  and  $C_{GBL}$  per area, and (c) heat capacities per one carrier  $c_{GL}$  and  $c_{GBL}$ , normalized by  $k_B$ , vs carrier temperature  $T$  at  $\mu = 0$  ( $\gamma_1 = 0.4$  eV).

at the Dirac point in GBLs), whereas the absence of the energy gap leads to a weak degeneracy near the Dirac point [ $f_e(0) = f_h(0) \simeq 1/2$ ]. In particular, if we would neglect the partial degeneracy effect, we obtain  $c_{GL} = 6$  and  $1 < c_{GBL} = (1 + 6k_B T/\gamma_1)/(1 + k_B T/\gamma_1) < 6$ , respectively.

The variation of  $\mu$  with the effective carrier temperature leads to a small modification of  $c_{GL}$  and  $c_{GBL}$  assuming a weak deviation from equilibrium. Depending on the pumping or heating conditions, this effect can result in either an increase or a decrease in  $\mu$  (see, for example, Ref. [14]) and, hence, in somewhat varying  $c_{GL}$  and  $c_{GBL}$ .

In the case when the gapless carrier density of states is given by a power energy dependence  $\rho(\varepsilon) \propto \varepsilon^\xi$ , for the heat capacity per a carrier  $c_\xi$ , one can obtain

$$\begin{aligned} c_\xi &= (\xi + 2) \frac{\int_0^\infty dx x^{\xi+1} [1 + \exp(x - \mu/k_B T)]^{-1}}{\int_0^\infty dx x^\xi [1 + \exp(x - \mu/k_B T)]^{-1}} \\ &= (\xi + 2) \frac{\mathcal{F}_{\xi+1}(\mu/k_B T)}{\mathcal{F}_\xi(\mu/k_B T)}. \end{aligned} \quad (16)$$

In particular, at  $\mu = 0$ , Eq. (16) yields

$$\begin{aligned} c_\xi &= (\xi + 2) \frac{\mathcal{F}_{\xi+1}(0)}{\mathcal{F}_\xi(0)} \\ &= (\xi + 2) \frac{\Gamma(\xi + 2)}{\Gamma(\xi + 1)} \frac{\zeta(\xi + 2)}{\zeta(\xi + 1)} \left[ \frac{1 - 1/2^{(\xi+1)}}{1 - 1/2^\xi} \right], \end{aligned} \quad (17)$$

where  $\Gamma(x)$  is the gamma function. For GLs ( $\xi = 1$ ) and GBLs ( $\xi = 0$ ,  $k_B T \ll \gamma_1$ ), from Eq. (17) we obtain  $c_{GL} = c_1 = 54\zeta(3)/\pi^2$  and  $c_{GBL} \simeq c_0 = \pi^2/6 \ln 2$ , that actually coincides with Eqs. (14) and (15).

The renormalization of the carrier spectrum and the density of states energy dependence in GLs, associated with the carrier-carrier interactions (for example, Refs. [6,44–49]), can somewhat affect the GL heat capacity. To estimate the role of the Fermi-liquid effect in GLs associated with the intercarrier interaction, following Ref. [47], in comparison with Eq. (1), we modify the carrier dispersion law in GLs as follows:

$$\varepsilon_{GL}^\pm = \pm v_W p \left[ 1 + g \ln \left( \frac{\mathcal{K}\hbar}{p} \right) \right]. \quad (18)$$

Here,  $g = e^2/(8\pi\hbar v_W \kappa)$  is the dimensionless carrier-carrier interaction parameter, where  $\kappa$  is the effective dielectric constant, and  $\mathcal{K}$  is the cutoff parameter [6,40,41] ( $\mathcal{K} \simeq 0.5 \times 10^8 \text{ cm}^{-1}$ ).

Considering Eq. (16), i.e., accounting for the carrier velocity renormalization, at  $\mu = 0$  for the renormalized carrier density  $\Sigma_{GL}^*$ , density of the carrier energy  $\mathcal{E}_{GL}^*$ , and the carrier heat capacity per one carrier  $c_{GL}$ , we obtain

$$r = \frac{\Sigma_{GL}^*}{\Sigma_{GL}} \simeq \frac{\mathcal{E}_{GL}^*}{\mathcal{E}_{GL}} \simeq \left[ 1 + g \ln \left( \frac{\mathcal{K}\hbar v_W}{k_B T} \right) \right]^{-2} < 1 \quad (19)$$

and

$$c_{GL}^* \simeq c_{GL}. \quad (20)$$

Setting  $\kappa = 2.5$ , at  $T = (10\text{--}300)$  K, we obtain  $r \simeq 0.59\text{--}0.72$ . One can see from Eq. (19) that the inclusion of the Fermi-liquid effect results in a natural lowering of the thermal carrier energy (due to a decrease in the density of states near the Dirac point), but, according to Eq. (20), this does not lead to a change in  $c_{GL}$ . Analogously, the inclusion into our model of the renormalization of the carrier dispersion law in the GBLs associated with the intercarrier interaction [50] also does not markedly affect  $c_{GBL}$ .

## V. CONCLUSIONS

We calculated the heat capacity per one carrier of the quasiequilibrium 2DEHP in GLs and GBLs and demonstrated that it can be larger from its classical values. The speed of operation (the switching time, turn-on time, and maximum modulation frequency) of the GL- and GBL-based devices, such as the bolometric photodetectors of terahertz and infrared radiation, electro-optical modulators, fast thermal radiation emitters, and superluminescent and lasing diodes, is affected by the carrier heating/cooling and is determined by the product of  $c_{GL}$  or  $c_{GBL}$  and the carrier energy relaxation time. Therefore, our results are important for the evaluation of the ultimate characteristics and optimization of such devices (see, for example, Ref. [51]).



## ACKNOWLEDGMENTS

The work at RIEC and UoA was supported by the Japan Society for Promotion of Science (KAKENHI Grant No. 20K20349) and the RIEC Nation-Wide Collaborative Research Project No. H31/A01, Japan. The work at RPI was supported by the Office of Naval Research (Project Man-

ager Dr. Paul Maki), the US Air Force Office of Scientific Research (Project No. FA9550-19-1-0355, Project Manager Dr. John Qiu), and the Army Research Laboratory under ARL MSME Alliance (Project Manager D. Meredith Reed), USA. The authors are grateful to A. Sergeev for useful comments.

- 
- [1] A. H. Castro Neto, F. Guinea, N. M. R. Peres, K. S. Novoselov, and A. K. Geim, The electronic properties of graphene, *Rev. Mod. Phys.* **81**, 109 (2009).
- [2] L. A. Falkovsky and S. S. Pershoguba, Optical far-infrared properties of graphene monolayer and multilayers, *Phys. Rev. B* **76**, 153410 (2007).
- [3] V. P. Gusynin, S. G. Sharapov, and J. P. Carbotte, Unusual Microwave Response of Dirac Quasiparticles in Graphene, *Phys. Rev. Lett.* **96**, 256802 (2006).
- [4] E. H. Hwang, S. Adam, and S. D. Sarma, Carrier Transport in Two-Dimensional Graphene Layers, *Phys. Rev. Lett.* **98**, 186806 (2007).
- [5] F. T. Vasko and V. Ryzhii, Voltage and temperature dependence of conductivity in gated graphene, *Phys. Rev. B* **76**, 233404 (2007).
- [6] E. G. Mishchenko, Effect of Electron-Electron Interactions on the Conductivity of Clean Graphene, *Phys. Rev. Lett.* **98**, 216801 (2007).
- [7] V. Ryzhii, M. Ryzhii, and T. Otsuji, Negative dynamic conductivity of graphene with optical pumping, *J. Appl. Phys.* **101**, 083114 (2007).
- [8] F. T. Vasko and V. Ryzhii, Photoconductivity of intrinsic graphene, *Phys. Rev. B* **77**, 195433 (2008).
- [9] O. G. Balev, V. T. Vasko, and V. Ryzhii, Carrier heating in intrinsic graphene by a strong dc electric field, *Phys. Rev. B* **79**, 165432 (2009).
- [10] O. Vafek, Thermoplasma Polariton with Scaling Theory of Single-Layer Graphene, *Phys. Rev. Lett.* **97**, 266406 (2006).
- [11] L. A. Falkovsky and A. A. Varlamov, Space-time dispersion of graphene conductivity, *Eur. Phys. J. B* **56**, 281 (2007).
- [12] V. Ryzhii, A. Satou, and T. Otsuji, Plasma waves in two-dimensional electron-hole system in gated graphene heterostructures, *J. Appl. Phys.* **101**, 024509 (2007).
- [13] S. Boubanga-Tombet, S. Chan, T. Watanabe, A. Satou, V. Ryzhii, and T. Otsuji, Ultrafast carrier dynamics and terahertz emission in optically pumped graphene at room temperature, *Phys. Rev. B* **85**, 035443 (2012).
- [14] V. Ryzhii, T. Otsuji, M. Ryzhii, V. E. Karasik, and M. S. Shur, Negative terahertz conductivity and amplification of surface plasmons in graphene-black phosphorus injection laser heterostructures, *Phys. Rev. B* **100**, 115436 (2019).
- [15] A. A. Balandin, S. Ghosh, W. Bao, I. Calizo, D. Teweldebrhan, F. Miao, and C. N. Lau, Superior thermal conductivity of single-layer graphene, *Nano Lett.* **8**, 902 (2008).
- [16] S. Ghosh, I. Calizo, D. Teweldebrhan, E. P. Pokatilov, D. L. Nika, A. A. Balandin, W. Bao, F. Miao, and C. N. Lau, Extremely high thermal conductivity of graphene: Prospects for thermal management applications in nanoelectronic circuits, *Appl. Phys. Lett.* **92**, 151911 (2008).
- [17] A. A. Balandin, Thermal properties of graphene and nanostructured carbon materials, *Nat. Mater.* **10**, 569 (2011).
- [18] E. Pop, V. Varshney, and A. K. Roy, Thermal properties of graphene: Fundamentals and applications, *MRS Bull.* **37**, 1273 (2012).
- [19] M. Sang, J. Shin, K. Kim, and K. J. Yu, Electronic and thermal properties of graphene and recent advances in graphene based electronics applications, *Nanomaterials (Basel)* **9**, 374 (2019).
- [20] L. X. Benedict, S. G. Louie, and M. L. Cohen, Heat capacity of carbon nanotubes, *Solid State Commun.* **100**, 177 (1996).
- [21] V. Ryzhii, M. Ryzhii, D. Ponomarev, V. G. Leiman, V. Mitin, M. Shur, and T. Otsuji, Negative photoconductivity and hot-carrier bolometric detection of terahertz radiation in graphene-phosphorene hybrid structures, *J. Appl. Phys.* **125**, 151608 (2019).
- [22] M. Shur, A. V. Muraviev, S. L. Rumyantsev, W. Knap, G. Liu, and A. A. Balandin, Plasmonic and bolometric terahertz graphene sensors, in *Proceedings of 2013 IEEE Sensors Conference (IEEE, Piscataway, NJ, 2013)*, pp. 1688–1690.
- [23] V. Ryzhii, T. Otsuji, M. Ryzhii, D. Ponomarev, V. Karasik, V. Leiman, V. Mitin, and M. Shur, Electrical modulation of terahertz radiation using graphene-phosphorene heterostructures, *Semicond. Sci. Technol.* **33**, 124010 (2018).
- [24] M. Freitag, H.-Y. Chiu, M. Steiner, V. Perebeinos, and P. Avouris, Thermal infrared emission from biased graphene, *Nat. Nanotechnol.* **5**, 497 (2010).
- [25] Y. D. Kim, H. Kim, Y. Cho, J. H. Ryoo, C.-H. Park, P. Kim, Y.-S. Kim, S. Lee, Y. Li, S.-N. Park, Y.-S. Yoo, D. Yoon, V. E. Dorgan, E. Pop, T. F. Heinz, J. Hone, S.-H. Chun, H. Cheong, S. W. Lee, M.-Ho Bae, and Y. D. Park, Bright visible light emission from graphene, *Nat. Nanotechnol.* **10**, 676 (2015).
- [26] H. R. Barnard, E. Zossimova, N. H. Mahlmeister, L. M. Lawton, I. J. Luxmoore, and G. R. Nash, Boron nitride encapsulated graphene infrared emitters, *Appl. Phys. Lett.* **108**, 131110 (2016).
- [27] S.-K. Son, M. Šiškins, C. Mullan, J. Yin, V. G. Kravets, A. Kozikov, S. Ozdemir, M. Alhazmi, M. Holwill, K. Watanabe, T. Taniguchi, D. Ghazaryan, K. S. Novoselov, V. I. Fal'ko, and A. Mishchenko, Graphene hot-electron light bulb: Incandescence from hBN encapsulated graphene in air, *2D Mater.* **5**, 011006 (2017).
- [28] H. M. Dong, W. Xu, and F. M. Peeters, Electrical generation of terahertz blackbody radiation from graphene, *Opt. Express* **26**, 24621 (2018).
- [29] F. Luo, Y. Fan, G. Peng, S. Xu, Y. Yang, K. Yuan, J. Liu, W. Ma, W. Xu, Z. H. Zhu, X.-A. Zhang, A. Mishchenko, Y. Ye, H. Huang, Z. Han, W. Ren, K. S. Novoselov, K. M. Zhu, and S. Qin, Graphene thermal emitter with enhanced Joule heating and localized light emission in air, *ACS Photonics* **6**, 2117 (2019).

- [30] Y. D. Kim, Y. Gao, R.-J. Shiue *et al.*, Ultrafast graphene light emitters, *Nano Lett.* **18**, 934 (2018).
- [31] V. Ryzhii, T. Otsuji, M. Ryzhii, V. Leiman, P. P. Maltsev, V. E. Karasik, V. Mitin, and M. S. Shur, Theoretical analysis of injection driven thermal light emitters based on graphene encapsulated by hexagonal boron nitride, *Opt. Mater. Express* **11**, 468 (2021).
- [32] V. Ryzhii, M. Ryzhii, T. Otsuji, V. E. Karasik, V. Leiman, V. Mitin, and M. S. Shur, Multiple graphene-layer-based heterostructures with van der Waals barrier layers for terahertz superluminescent and laser diodes with lateral/vertical current injection, *Semicond. Sci. Technol.* **35**, 085023 (2020).
- [33] R. Yu, A. Manjavacas, and F. J. García de Abajo, Ultrafast radiative heat transfer, *Nat. Commun.* **8**, 2 (2017).
- [34] E. J. C. Dias, R. Yu, and F. J. García de Abajo, Thermal manipulation of plasmons in atomically thin films, *Light: Sci. Appl.* **9**, 87 (2020).
- [35] E. McCann and V. Falko, Landau-Level Degeneracy and Quantum Hall Effect in a Graphite Bilayer, *Phys. Rev. Lett.* **96**, 086805 (2006).
- [36] E. McCann, D. S. L. Abergel, and V. I. Fal'ko, The low energy electronic band structure of bilayer graphene, *Eur. Phys. J. Spec. Top.* **148**, 91 (2007).
- [37] C. H. Lui, K. F. Mak, J. Shan, and T. F. Heinz, Ultrafast Photoluminescence from Graphene, *Phys. Rev. Lett.* **105**, 127404 (2010).
- [38] J. C. W. Song, K. J. Tielrooij, F. H. L. Koppens, and L. S. Levitov, Photoexcited carrier dynamics and impact-excitation cascade in graphene, *Phys. Rev. B* **87**, 155429 (2013).
- [39] J. C. Johannsen, S. Ulstrup, F. Cilento, A. Crepaldi, M. Zacchigna, C. Cacho, I. C. E. Turcu, E. Springate, F. Fromm, C. Roidel, T. Seyller, F. Parmigiani, M. Grioni, and P. Hofmann, Direct View of Hot Carrier Dynamics in Graphene, *Phys. Rev. Lett.* **111**, 027403 (2013).
- [40] S. A. Mikhailov, Theory of the strongly nonlinear electrodynamic response of graphene: A hot electron model, *Phys. Rev. B* **100**, 115416 (2019).
- [41] X. Li, E. A. Barry, J. M. Zavada, M. Buongiorno Nardelli, and K. W. Kim, Influence of electron-electron scattering on transport characteristics in monolayer graphene, *Appl. Phys. Lett.* **97**, 082101 (2010).
- [42] G. Alymov, V. Vyurkov, V. Ryzhii, A. Satou, and D. Svintsov, Auger recombination in Dirac materials: A tangle of many-body effects, *Phys. Rev. B* **97**, 205411 (2018).
- [43] M. S. Foster and I. L. Aleiner, Slow imbalance relaxation and thermoelectric transport in graphene, *Phys. Rev. B* **79**, 085415 (2009).
- [44] D. C. Elias, R. V. Gorbachev, A. S. Mayorov, S. V. Morozov, A. A. Zhukov, P. Blake, L. A. Ponomarenko, I. V. Grigorieva, K. S. Novoselov, F. Guinea, and A. K. Geim, Dirac cones reshaped by interaction effects in suspended graphene, *Nat. Phys.* **7**, 701 (2011).
- [45] G. L. Yu, R. Jalil, B. Belle, A. S. Mayorov, P. Blake, F. Schedin, S. V. Morozov, L. A. Ponomarenko, F. Chiappini, S. Wiedmann, U. Zeitler, M. I. Katsnelson, A. K. Geim, K. S. Novoselov, and D. C. Elias, Interaction phenomena in graphene seen through quantum capacitance, *Proc. Natl. Acad. Sci. USA* **110**, 3282 (2013).
- [46] J. Gonzalez, F. Guinea, and M. A. H. Vozmediano, Marginal-Fermi-liquid behavior from two-dimensional Coulomb interaction, *Phys. Rev. B* **59**, R2474(R) (1999).
- [47] L. A. Falkovsky, Thermodynamics of electron-hole liquids in graphene, *JETP Lett.* **98**, 161 (2013).
- [48] H.-K. Tang, J. N. Leaw, J. N. B. Rodrigues, I. F. Herbut, P. Sengupta, F. F. Assaad, and S. Adam, The role of electron-electron interactions in two-dimensional Dirac fermions, *Science* **361**, 570 (2018).
- [49] V. N. Kotov, B. Uchoa, V. M. Pereira, F. Guinea, and A. H. Castro Neto, Electron-electron interactions in graphene: Current status and perspectives, *Rev. Mod. Phys.* **84**, 1067 (2012).
- [50] S. V. Kusminskiy, D. K. Campbell, and A. H. Castro Neto, Electron-electron interactions in graphene bilayers, *Europhys. Lett.* **85**, 58005 (2009).
- [51] V. Ryzhii, M. Ryzhii, T. Otsuji, V. Leiman, V. Mitin, and M. S. Shur, Modulation characteristics of uncooled graphene photodetectors, *J. Appl. Phys.* **129**, 000000 (2021).